NATIONAL ADVISORY COMMITTEE FOR AERONAUTICS

TECHNICAL NOTE 2151

ESTIMATION OF THE DAMPING IN ROLL OF SUPERSONIC-LEADING-EDGE WING-BODY COMBINATIONS

By Warren A. Tucker and Robert O. Piland

Langley Aeronautical Laboratory
Langley Air Force Base, Va.

NACA

Washington
July 1950

NATIONAL ADVISORY COMMITTEE FOR AERONAUTICS

TECHNICAL NOTE 2151

ESTIMATION OF THE DAMPING IN ROLL OF SUPERSONIC-LEADING-EDGE WING-BODY COMBINATIONS

By Warren A. Tucker and Robert O. Piland

SUMMARY

A description is given of a linear-theory method for the estimation of the damping in roll of supersonic-leading-edge wings mounted on cylindrical bodies. The error resulting from an approximation essential to the method is shown to be small.

The damping in roll is calculated for configurations having rectangular and triangular wings; for most of the range of variables the net effect of the body is to decrease the damping in roll. The body effect is small for body diameters less than about 30 percent of the wing span but increases rapidly with body size above this value.

INTRODUCTION

The damping in roll of wings of various plan forms in supersonic flight has been the subject of several investigations. The theory for the isolated wing is well-advanced; in connection with the present work the results for the rectangular wing (references 1 and 2) and the triangular wing (reference 3) are of interest. In actual aircraft, however, the wing is commonly mounted on a body so that a method of evaluating the effect of the body is desirable for the purpose of applying isolated-wing theory to practical cases.

The present paper describes a linear-theory method for estimating the damping in roll of thin supersonic-leading-edge wings mounted on cylindrical bodies. The method is applied to the calculation of the damping in roll of configurations having rectangular and triangular wings. The triangular-wing configuration with a subsonic leading edge has been treated by other investigators in reference 4.

The accuracy of the method in determining the pressure distribution in the region of the wing affected by the presence of the body is difficult to assess, but within the range of applicability of the method

(small wing thicknesses, no viscous effects) the error in total rolling moment can be shown to be small.

SYMBOLS

s	distance from body center line to wing tip
a	radius of cylindrical body
p	rolling angular velocity, positive when clockwise viewed from rear
$b = 2s$	
h	distance from body center line to limit of juncture region (see fig. 1)
V	free-stream velocity
M	free-stream Mach number
$\beta = \sqrt{M^2 - 1}$	
$pb/2V$	wing-tip helix angle
q	free-stream dynamic pressure
S	wing area, including the part of the wing covered by the body
L	rolling moment, positive when acting clockwise viewed from rear
C_l	rolling-moment coefficient $\left(\frac{L}{qSb}\right)$
C_{l_p}	damping-in-roll derivative $\left(\frac{\partial C_l}{\partial \frac{pb}{2V}}\right)$
$\left(C_{l_p}\right)_W$	damping-in-roll derivative for isolated wing
A	aspect ratio (b^2/S)
x,y	coordinates for field points (see fig. 2)

ξ,η coordinates for source points (see fig. 2)

G local source strength

ϕ disturbance-velocity potential

$\phi_x = \frac{\partial \phi}{\partial x}$

k slope of leading edge (see fig. 2)

$m = \frac{1}{k}$

P pressure difference between upper and lower surfaces

C_p pressure coefficient $\left(\frac{P}{q}\right)$

ANALYSIS

The basis of the analysis is the representation of the rolling wing and body by a distribution of sources chosen so as to satisfy approximately the boundary conditions of the problem. After this distribution has been chosen, the determination of the resulting pressure distribution and rolling moment is straightforward, although somewhat lengthy.

Source distribution.- The geometry of the rolling wing-body system is shown in figure 1(a). The part of the fuselage to which the wing is attached is assumed to be a cylinder of radius a, and the whole system is rolling at an angular velocity p.

The right wing, for example, can be replaced by a distribution of point sources the strengths of which are equal to $1/\pi$ times the local vertical velocity (reference 5). For the present case, then, the source strength is directly proportional to the distance from the body center line (see fig. 1(b)).

The boundary condition to be satisfied on the body is, of course, that there be no flow normal to the body. In order to satisfy this condition, the source distribution necessary to represent the body must be such that it acts together with the source distribution for the wing to produce a flow which has no component normal to the body. The determination of such a source distribution would be a very difficult task, and the distribution when found would very likely be so complicated as to

present further difficulties in the succeeding steps. An approximation is therefore in order.

Consider the case for which the body radius is only slightly less than the distance h (see fig. 1(a)). For this condition the effect of the body on the wing will be much the same as that of a large flat plate mounted normal to the wing along the wing-body juncture. The source distribution required to represent this flat plate is simply that shown in figure 1(c). As the size of the body relative to the distance h is decreased the effect of the body becomes less and less like that of a flat plate until finally the source distribution is simply that for the wing alone (see fig. 1(d)).

This knowledge of the conditions at the end points has been used to select a source distribution which represents the effect of the body in an approximate manner. The chosen distribution is shown in figure 1(e); the slope of the distribution curve varies linearly with a/h. This distribution is at best a crude approximation to the actual state so far as the boundary condition on the body is concerned. However, as shown in the section entitled "Discussion," the resulting error in rolling moment is small.

Pressure distribution.- The source distribution being chosen, the method of reference 5 can be used to find the pressure distribution in the wing area between the wing-body juncture and the Mach line from the leading edge of the juncture. This area is hereinafter called the juncture region. This region is the only one in which the pressure need be determined and in which the body effect is felt directly; the pressures acting on the body are quite ineffective in producing rolling moments and the pressures over the other areas of the wing are known from references 1 to 3.

The source distribution of figure 1(e) is sufficient to show that, at least for the rectangular-wing case, the pressure in the juncture region has a greater absolute value than would be the case were the body not present. The corresponding increase in damping, however, is opposed by the decrease which results from covering part of the wing with the body. The relative magnitudes of the two effects cannot be evaluated from qualitative reasoning.

The axis system for the determination of the pressure in the juncture region is shown in figure 2. The disturbance-velocity potential at a point (x,y) is given by

$$\phi = -\iint Gf(\xi,\eta)\, d\xi\, d\eta \qquad (1)$$

where G is the local source strength, the integration is over the entire shaded area in figure 2, and

$$f(\xi,\eta) = \left[(x - \xi)^2 - \beta^2(y - \eta)^2\right]^{-1/2}$$

The integration is most conveniently carried out over the three separate shaded areas in figure 2 so that equation (1) becomes

$$-\frac{\pi}{p}\phi = \int_{y}^{\frac{\beta y+x}{\beta+k}} \int_{k\eta}^{x+\beta y-\beta\eta} (a + \eta) f(\xi,\eta)\, d\xi\, d\eta +$$

$$\int_{0}^{y} \int_{k\eta}^{x-\beta y+\beta\eta} (a + \eta) f(\xi,\eta)\, d\xi\, d\eta +$$

$$\int_{\frac{\beta y-x}{\beta+k}}^{0} \int_{-k\eta}^{x-\beta y+\beta\eta} \left[a - \left(2\frac{a}{h} - 1\right)\eta\right] f(\xi,\eta)\, d\xi\, d\eta \qquad (2)$$

The first integration with respect to ξ gives

$$-\frac{\pi}{p}\phi = \int_{0}^{\frac{\beta y+x}{\beta+k}} (a + \eta) \cosh^{-1}\left|\frac{x - k\eta}{\beta(y - \eta)}\right| d\eta +$$

$$\int_{\frac{\beta y-x}{\beta+k}}^{0} \left[a - \left(2\frac{a}{h} - 1\right)\eta\right] \cosh^{-1}\left|\frac{x + k\eta}{\beta(y - \eta)}\right| d\eta \qquad (3)$$

The partial derivative ϕ_x is necessary for the determination of the pressure. This derivative is found most conveniently at this point in the analysis by differentiation under the integral sign. This operation results in

$$-\frac{\pi}{p}\phi_x = \int_0^{\frac{\beta y+x}{\beta+k}} \frac{(a+\eta)\,d\eta}{\sqrt{x^2-\beta^2y^2+(2\beta^2y-2kx)\eta-(\beta^2-k^2)\eta^2}} + \int_{\frac{\beta y-x}{\beta+k}}^{0} \frac{\left[a-\left(2\frac{a}{h}-1\right)\eta\right]d\eta}{\sqrt{x^2-\beta^2y^2+(2\beta^2y+2kx)\eta-(\beta^2-k^2)\eta^2}} \tag{4}$$

These integrals are easily evaluated. If a pressure coefficient is defined as

$$C_p = \frac{P}{q} \tag{5}$$

where P is the pressure difference between the upper and lower surfaces, then

$$C_p = -\frac{4}{V}\phi_x \tag{6}$$

Substitution of equation (4) into equation (6) results in

$$C_p\frac{V\pi}{4p} = \left(2\frac{a}{h}-1\right)\frac{\sqrt{x^2-\beta^2y^2}}{\beta^2-k^2} + \frac{\sqrt{x^2-\beta^2y^2}}{\beta^2-k^2} + \frac{a}{\sqrt{\beta^2-k^2}}\left[\cos^{-1}\frac{kx-\beta^2y}{\beta(x-ky)} + \cos^{-1}\frac{kx+\beta^2y}{\beta(x+ky)}\right] + \frac{\beta^2y-kx}{(\beta^2-k^2)^{3/2}}\cos^{-1}\frac{kx-\beta^2y}{\beta(x-ky)} - \left(2\frac{a}{h}-1\right)\frac{\beta^2y+kx}{(\beta^2-k^2)^{3/2}}\cos^{-1}\frac{kx+\beta^2y}{\beta(x+ky)} \tag{7}$$

This equation gives the pressure coefficient acting over the region of the wing affected by the body; as has been mentioned before, the pressures acting over the other areas are known from references 1 to 3.

For the rectangular-wing case, k is put equal to zero. The quantity $\left(2\frac{a}{h} - 1\right)$ can be expressed in terms of more familiar parameters. For the rectangular wing:

$$2\frac{a}{h} - 1 = \frac{\frac{a}{s} - \frac{2}{\beta A}}{\frac{a}{s} + \frac{2}{\beta A}}$$

and for the triangular wing:

$$2\frac{a}{h} - 1 = \frac{\left(\frac{\beta A}{4} + 1\right)\frac{a}{s} - 1}{\left(\frac{\beta A}{4} - 1\right)\frac{a}{s} + 1}$$

Damping-in-roll derivative.- The damping-in-roll derivative Cl_p is found for either the triangular or the rectangular plan form by suitable integration of the various pressure distributions. The rather lengthy integrations are not included here. The wing area and span upon which the coefficient is based include those parts of the wing masked by the body.

The result for the rectangular-wing configuration is given by the following equation:

$$-\beta Cl_p = \frac{2}{3} - \frac{1}{\beta A} + \frac{1}{3(\beta A)^2} + \frac{1}{12(\beta A)^3} - \frac{2\frac{a}{s}}{3\left(\frac{a}{s} + \frac{2}{\beta A}\right)}\left[\left(\frac{a}{s}\right)^3 + \frac{2}{\beta A}\left(\frac{a}{s}\right)^2 - \frac{1}{(\beta A)^2}\frac{a}{s} - \frac{4}{3\pi(\beta A)^3}\right] \quad (8)$$

This equation reduces correctly to the equation for the isolated wing (references 1 and 2) if a/s is put equal to zero. The equation is valid whether or not the Mach lines cross each other, so long as the Mach line from the leading edge of the wing-body juncture does not cross the wing tip. This condition can be expressed mathematically by the expression

$$\frac{a}{s} \leq 1 - \frac{2}{\beta A} \quad (9)$$

The corresponding result for the triangular-wing configuration is given by the following equation:

$$-\beta C_{l_p} = \frac{\frac{a}{s}\left(1 - \frac{a}{s}\right)^3}{3\pi\left[\left(\frac{\beta A}{4} - 1\right)\frac{a}{s} + 1\right]}\left(\frac{\frac{\beta A}{4}\cos^{-1}\frac{4}{\beta A}}{\left[\left(\frac{\beta A}{4}\right)^2 - 1\right]^{3/2}}\left\{2\left(\frac{\beta A}{4}\right)^3\left(1 + \frac{a}{s}\right) + \left[8\left(\frac{\beta A}{4}\right)^2 - 12\right]\left(1 - \frac{a}{s}\right) - \frac{\beta A}{4}\left(3 + \frac{a}{s}\right)\right\} + \frac{4}{\beta A\left[\left(\frac{\beta A}{4}\right)^2 - 1\right]}\left\{2\left(\frac{\beta A}{4}\right)^3\left(1 + \frac{a}{s}\right) + \left[8\left(\frac{\beta A}{4}\right)^2 - 4\right]\left(1 - \frac{a}{s}\right) - \frac{\beta A}{4}\left(1 + 3\,\frac{a}{s}\right)\right\} + \frac{\pi}{\frac{a}{s}\left(1 - \frac{a}{s}\right)}\left\{2\,\frac{\beta A}{4}\left[2\left(\frac{a}{s}\right)^3 + \left(\frac{a}{s}\right)^2\right] + \left(1 - \frac{a}{s}\right)\left[1 - 2\,\frac{a}{s} + 7\left(\frac{a}{s}\right)^2\right]\right\}\right) \tag{10}$$

Substitution of $\frac{a}{s} = 0$ causes all but one term to vanish. The value 1/3 given by this term is the correct value for the isolated wing (reference 3). The only restriction on equation (10) is that the Mach line from the leading edge of the wing-body juncture must be behind the leading edge of the wing $\left(\frac{\beta A}{4} \geq 1\right)$. As βA approaches infinity, equation (10) becomes

$$-\beta C_{l_p} = \frac{1}{3}\left[1 - 4\left(\frac{a}{s}\right)^3 + 3\left(\frac{a}{s}\right)^4\right] \tag{11}$$

DISCUSSION

Effect of approximate source distribution.- In the preceding analysis, the presence of the body has been represented by a rather arbitrarily selected source distribution. The error arising from this approximation should therefore be examined so that the validity of the results can be assessed. One method of evaluating the error is to determine how closely the boundary condition of no flow normal to the body is met by the velocity field induced by the source distribution of

figure 1(e). If this approach is adopted, it is not difficult to show that the maximum value of v_n/V is of order $(pb/2V)(a/s)$, where v_n is the velocity normal to the body. However interesting this result may be from an academic point of view, it supplies no direct answer to the more practical question of how much error can be expected in the estimated value of C_{l_p} for a given wing on a given body.

The maximum possible error in C_{l_p} can be determined by the consideration of two extreme cases. As one extreme, the slope of the source distribution representing the effect of the body can be taken equal to p/π, regardless of the body size (see fig. 1(e)). This case will give the maximum possible value of C_{l_p} (the physical interpretation is that the effect of the body is taken as that of a large flat plate mounted normal to the wing along the wing-body juncture). As the other extreme, the slope of the source distribution representing the effect of the body can be taken equal to $-p/\pi$, again without regard to body size. This case, which will result in the minimum value of C_{l_p}, can be regarded for the rectangular-wing configuration as an assumption that the body has no effect on the part of the wing outside the body. As simple a physical interpretation is not possible for the triangular-wing case. The difference between the two values of C_{l_p} will of course be the maximum possible error.

The pressure distribution in the juncture region for these two extreme cases is shown in figure 3 for a particular set of rectangular wing-body combinations, together with the pressure distribution given by the present approximation. The inference is clear that large errors in span load distribution are possible, particularly at stations close to the wing-body juncture. The error in C_{l_p}, however, is not necessarily large, because of the relative nearness of the juncture region (compared with the outer parts of the wing) to the moment axis (body center line). That the error in C_{l_p} for the rectangular-wing case is, in fact, acceptably small for engineering purposes is demonstrated by the curves of figure 4, which is self-explanatory. The information corresponding to that shown in figure 4 for the rectangular-wing case is given in figure 5 for the triangular wing; the error in C_{l_p} is again small.

Rectangular wing.- Now that the error introduced by the use of an approximate source distribution has been shown to be small, the results of calculations made with the use of equations (8), (10), and (11) may be discussed. The effect of body size on the damping in roll of rectangular-wing configurations is shown in figures 6 and 7. The question posed in the section entitled "Pressure distribution," namely whether the effect of covering part of the wing with a body or the effect of the increased damping in the juncture region is predominant,

is here resolved; the effect of covering part of the wing is the greater for most of the range of variables. The net effect of the body is not very important, however, for values of a/s less than about 0.3. The curves of figure 7 show that the percentile effect of the body is not greatly dependent upon βA.

Triangular wing.- The effect of body size on the damping in roll of triangular-wing configurations is shown in figure 8. As was the case for the rectangular wing, the net effect of the body is generally to decrease the damping in roll, although some opposite effect is present for small values of a/s.

The percentile effect of the body for the triangular-wing case is shown in figure 9, which corresponds to figure 7 for the rectangular-wing case. In contrast to the rectangular-wing case, the value of βA has an appreciable influence on the magnitude of the body effect. The curve for $\frac{\beta A}{4} \longrightarrow 0$ is taken from reference 4; the value $\frac{\beta A}{4} \longrightarrow 0$ refers physically to the condition that the wing leading edge is highly swept back relative to the Mach lines.

Other considerations.- Although the damping-in-roll derivative Cl_p has been worked out only for rectangular and triangular plan forms, the pressure coefficient in the juncture region given by equation (7) is equally applicable to any other plan form with a straight supersonic leading edge. There is also little doubt that the results may be applied, within the accuracy of the present analysis, to configurations having bodies which are not true cylinders, but which are almost cylindrical (quasi-cylindrical).

There are at least three limitations inherent in the analysis. The first is, of course, the use of an approximate source distribution to represent the body effect; the attendant errors have been discussed in the first part of this section. The second is the assumption of vanishingly small wing thickness. The effect of moderate thickness in the absence of viscosity may be expected to be small (see, for example, reference 6). The third, and possibly most severe, limitation is the assumption of an inviscid fluid. The magnitude of this error is practically impossible to evaluate theoretically, and there is not yet much applicable experimental data.

CONCLUDING REMARKS

A linear-theory method for the estimation of the effect of a cylindrical body on the damping in roll of wings with supersonic leading

edges is presented. The essential feature of the method is the representation of the effect of the body on the wing by a rather arbitrarily chosen source distribution. The error in damping in roll which could result from this procedure is shown to be small.

The damping in roll is calculated for configurations having rectangular and triangular wings. The body effect is found to be small for body diameters less than about 30 percent of the wing span but increases rapidly with body size above this value.

The results for the supersonic-leading-edge triangular-wing case are compared with those obtained by other investigators for the subsonic-leading-edge case. The leading-edge condition is shown to be an important parameter.

Langley Aeronautical Laboratory
National Advisory Committee for Aeronautics
Langley Air Force Base, Va., April 12, 1950

REFERENCES

1. Lagerstrom, P. A., and Graham, Martha E.: Some Aerodynamic Formulas in Linearized Supersonic Theory for Damping in Roll and Effect of Twist for Trapezoidal Wings. Rep. No. SM-13200, Douglas Aircraft Co., Inc., March 12, 1948.

2. Harmon, Sidney M.: Stability Derivatives at Supersonic Speeds of Thin Rectangular Wings with Diagonals ahead of Tip Mach Lines. NACA Rep. 925, 1949.

3. Brown, Clinton E., and Adams, Mac C.: Damping in Pitch and Roll of Triangular Wings at Supersonic Speeds. NACA Rep. 892, 1948.

4. Lomax, Harvard, and Heaslet, Max. A.: Damping-in-Roll Calculations for Slender Swept-Back Wings and Slender Wing-Body Combinations. NACA TN 1950, 1949.

5. Puckett, Allen E.: Supersonic Wave Drag of Thin Airfoils. Jour. Aero. Sci., vol. 13, no. 9, Sept. 1946, pp. 475-484.

6. Ivey, H. Reese: Notes on the Theoretical Characteristics of Two-Dimensional Supersonic Airfoils. NACA TN 1179, 1947.

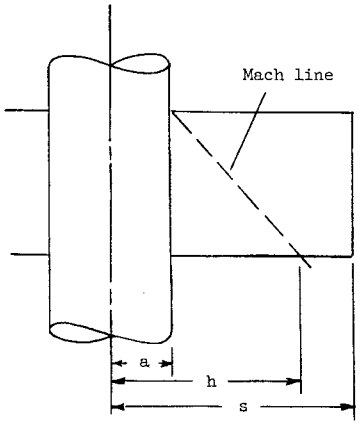

Plan view - rectangular wing

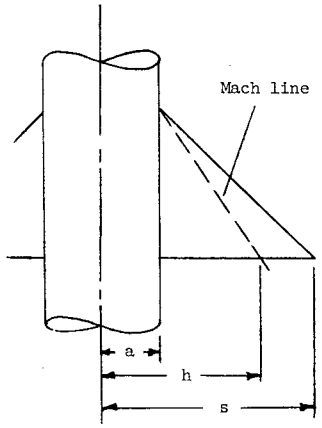

Plan view - triangular wing

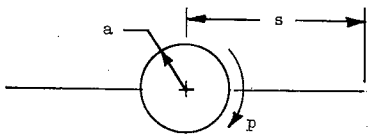

Rear view

(a) The wing-body system.

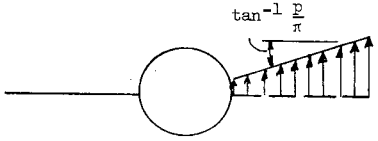

(b) Source representation of right wing.

(c) Source representation of body and right wing for $\frac{a}{h} \to 1$.

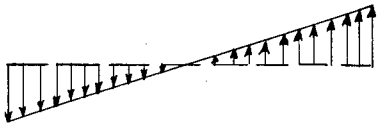

(d) Source representation of wing alone $\left(\frac{a}{h} = 0\right)$.

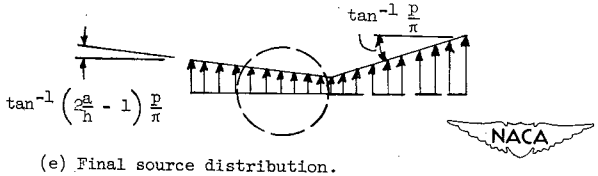

(e) Final source distribution.

Figure 1.- Steps in choice of source distribution.

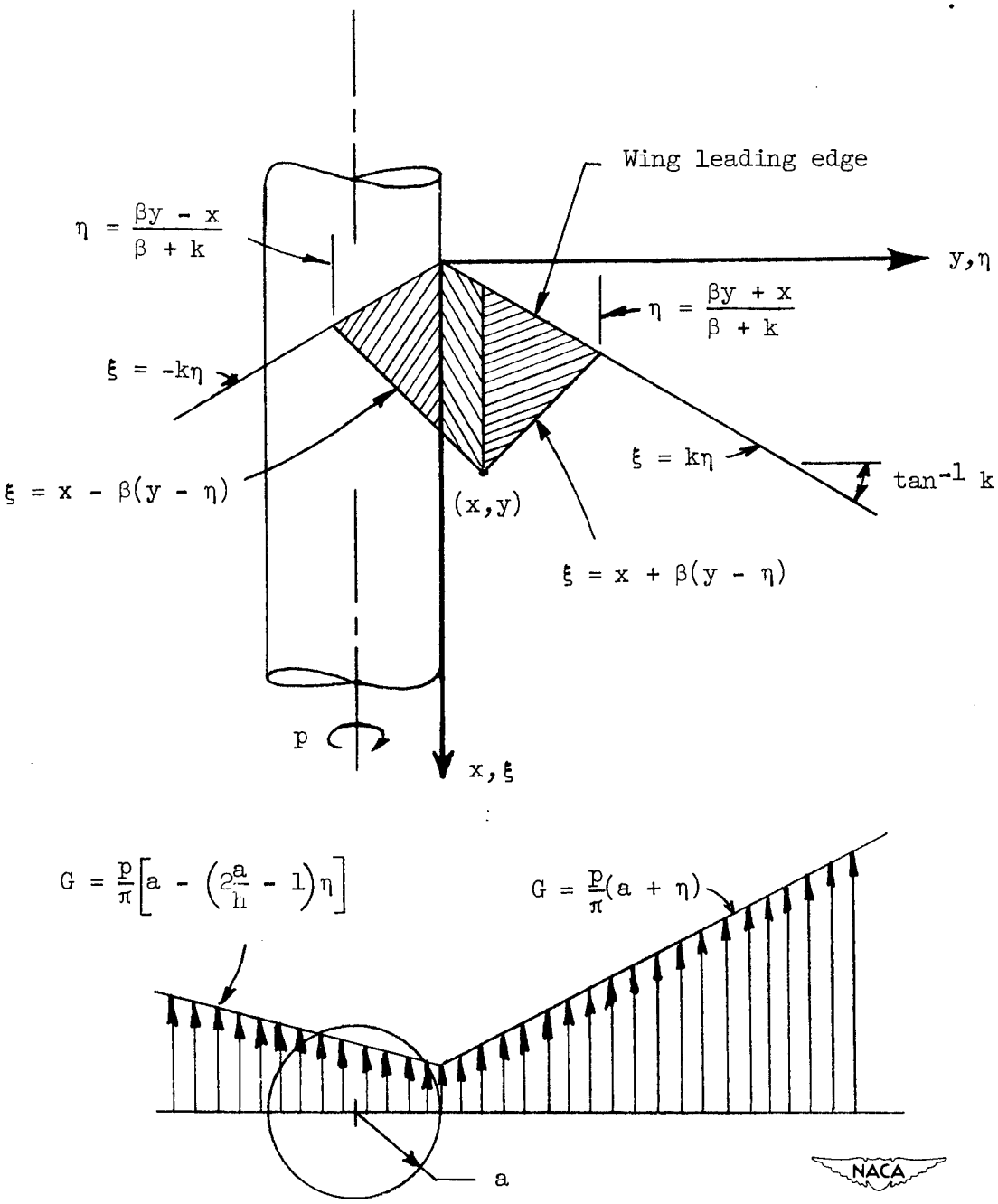

Figure 2.- Axis system.

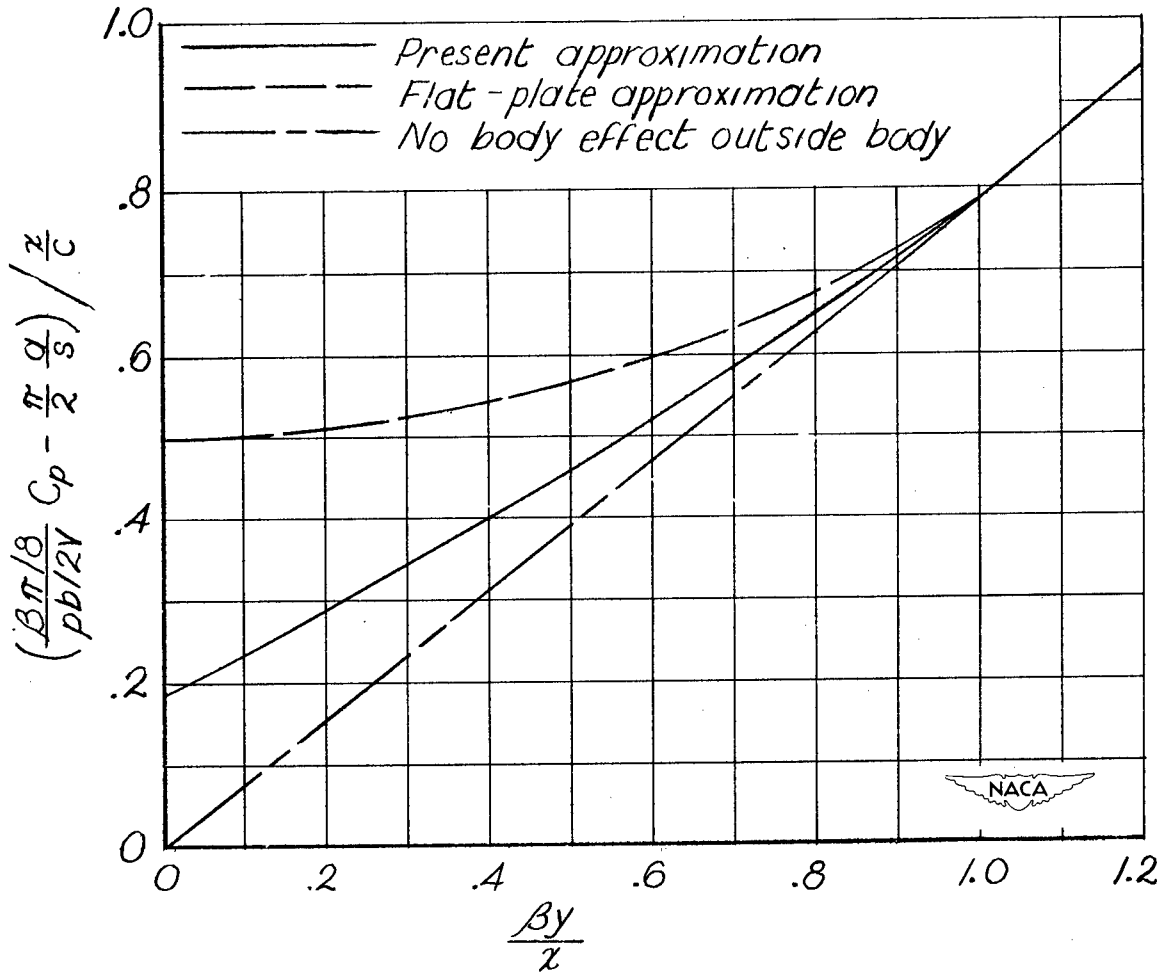

Figure 3.- Various approximations to pressure in juncture region. Rectangular wing-body combination. $\frac{a}{s} = 0.3$; $\beta A = 4$.

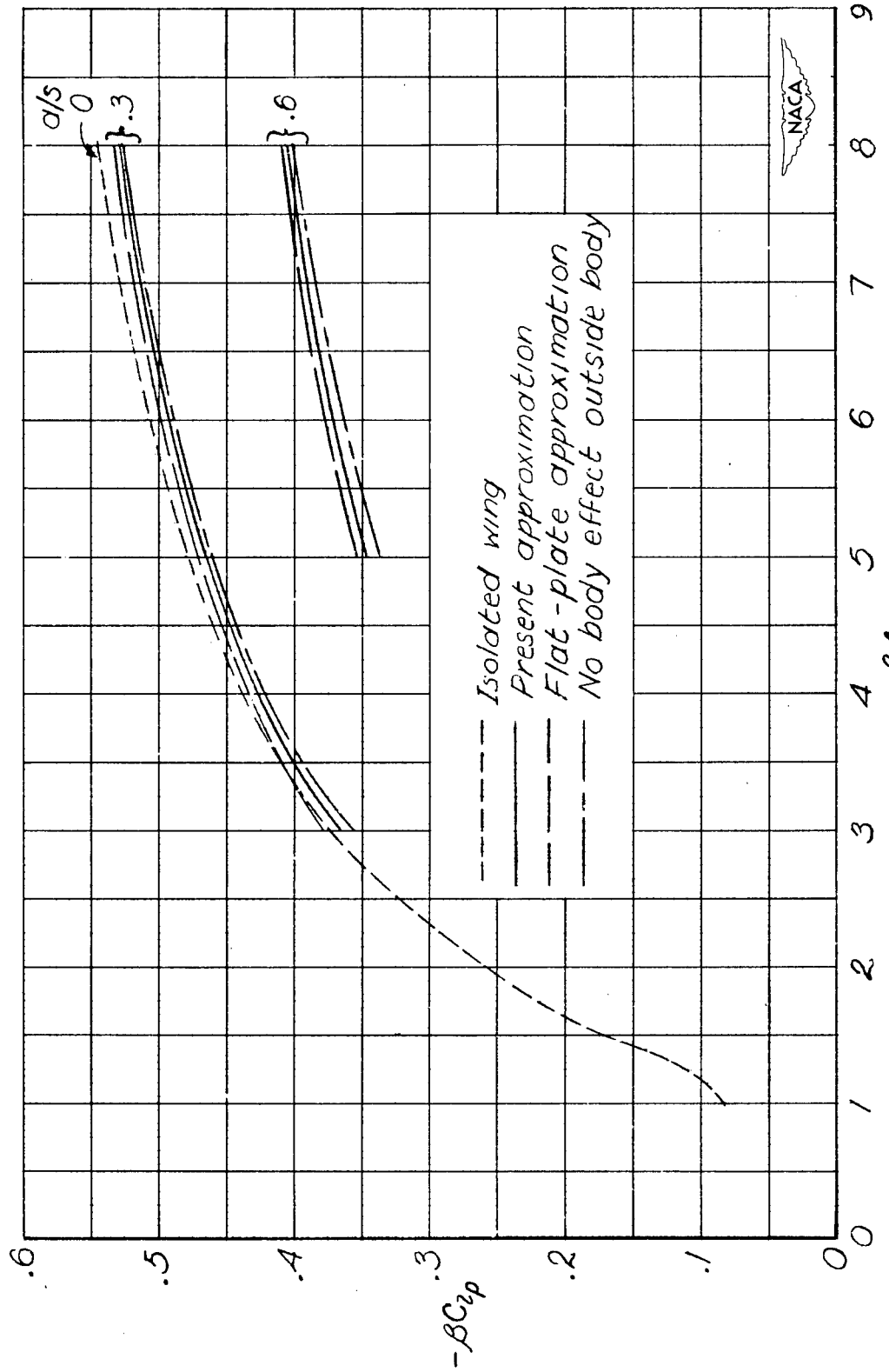

Figure 4.- Effect of various approximations to pressure in juncture region. Rectangular wing-body combination.

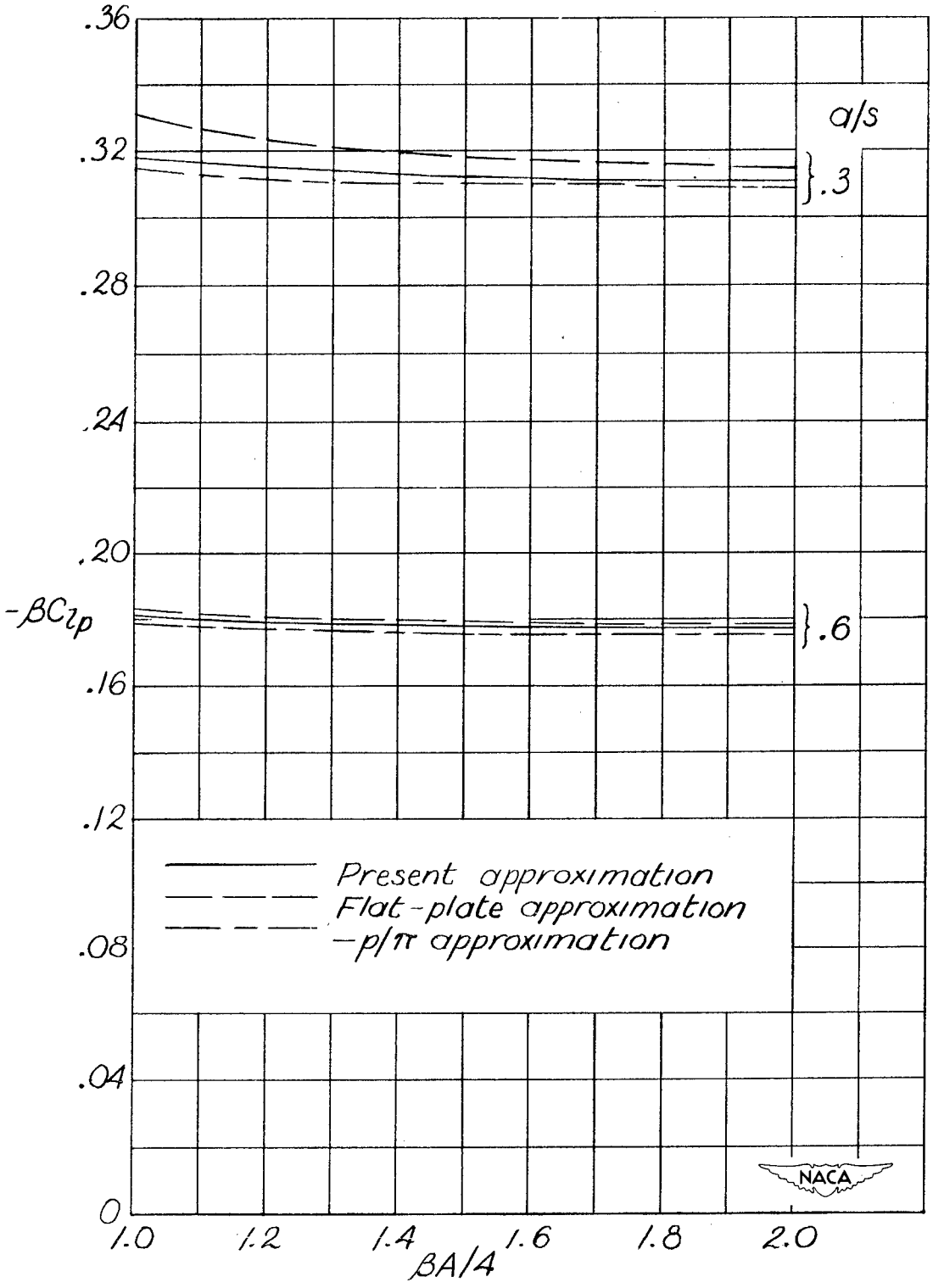

Figure 5.- Effect of various approximations to pressure in juncture region. Triangular wing-body combination.

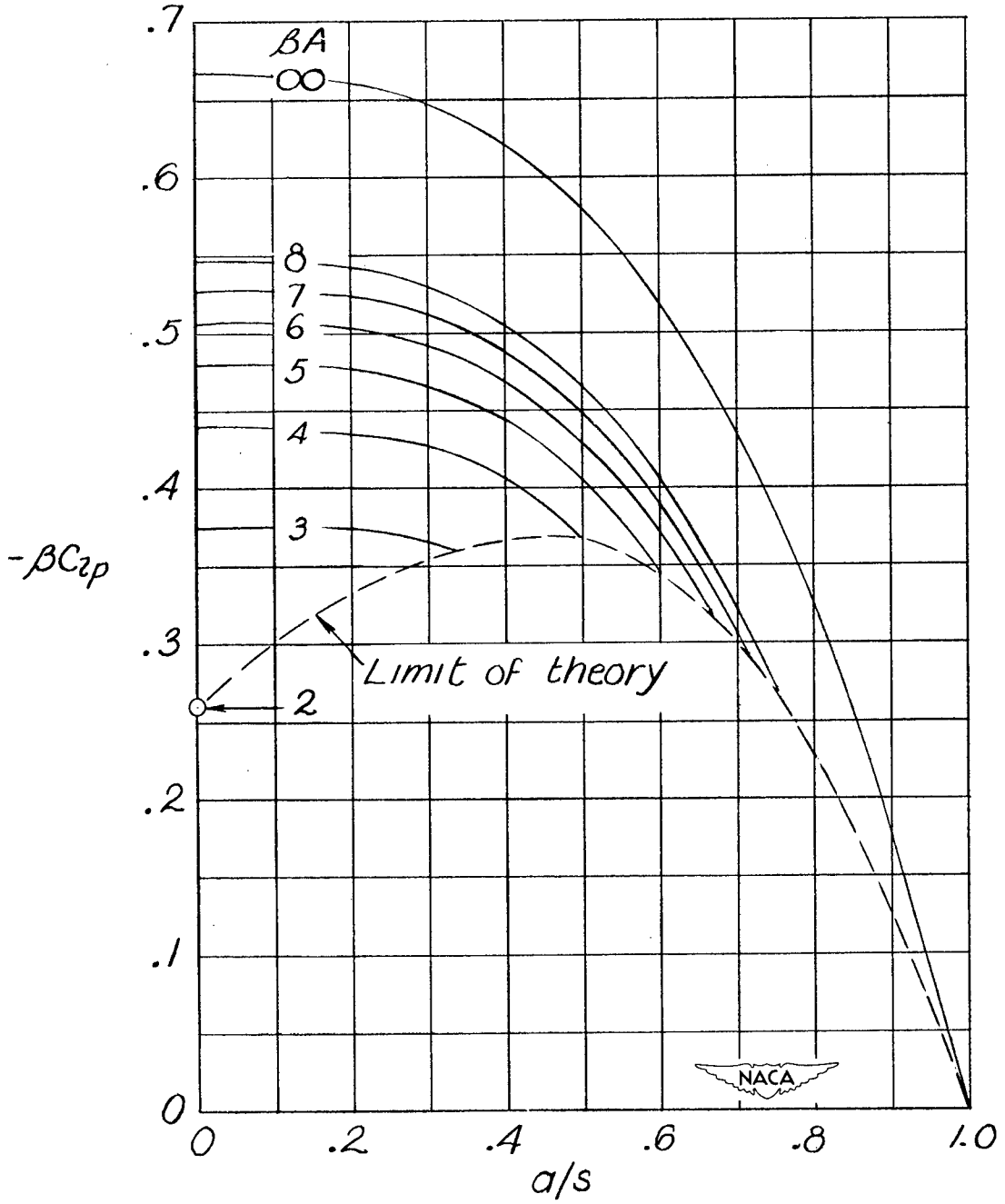

Figure 6.- Damping in roll of rectangular wings on cylindrical bodies.

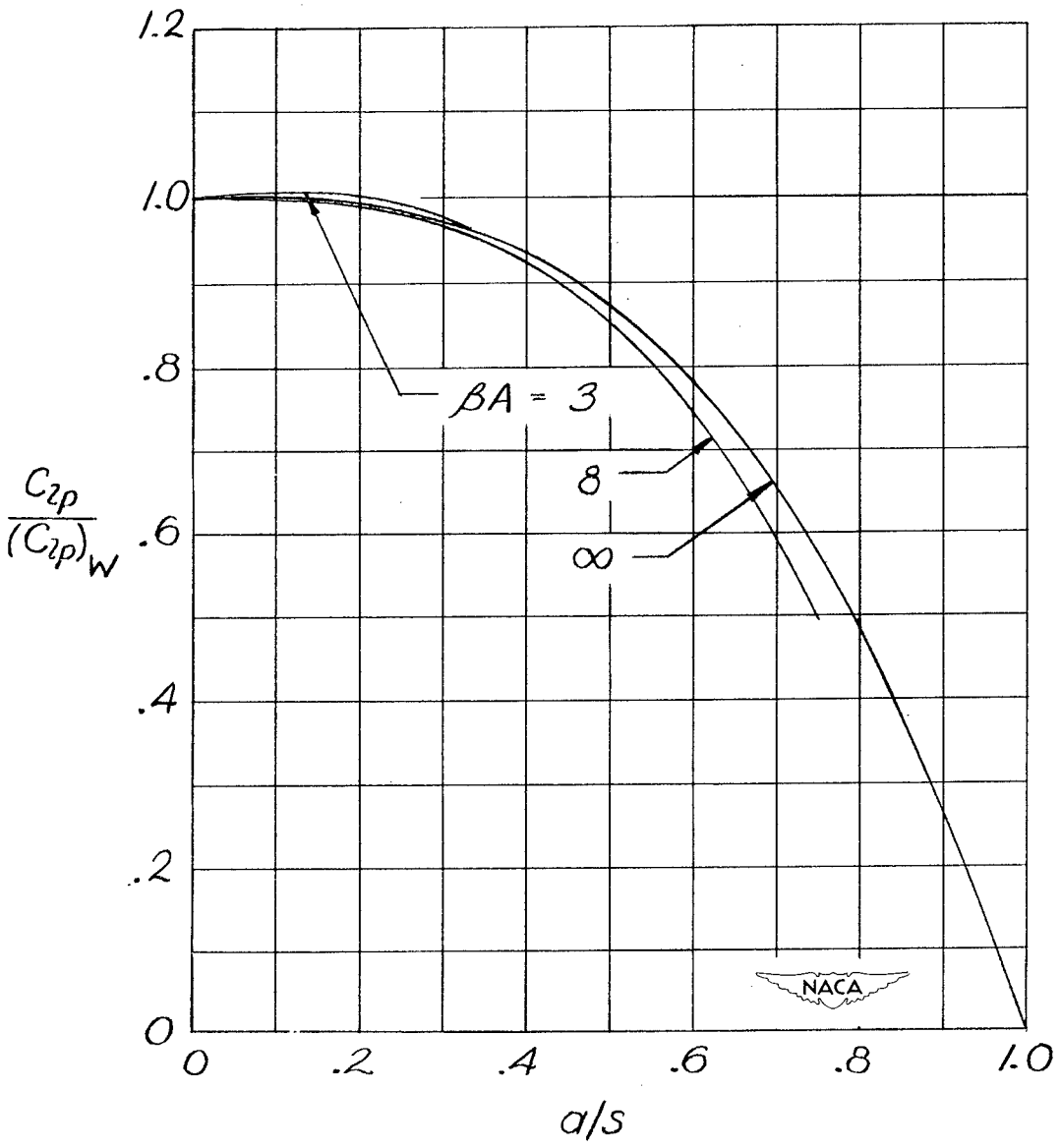

Figure 7.- Relative effect of body for rectangular-wing configurations.

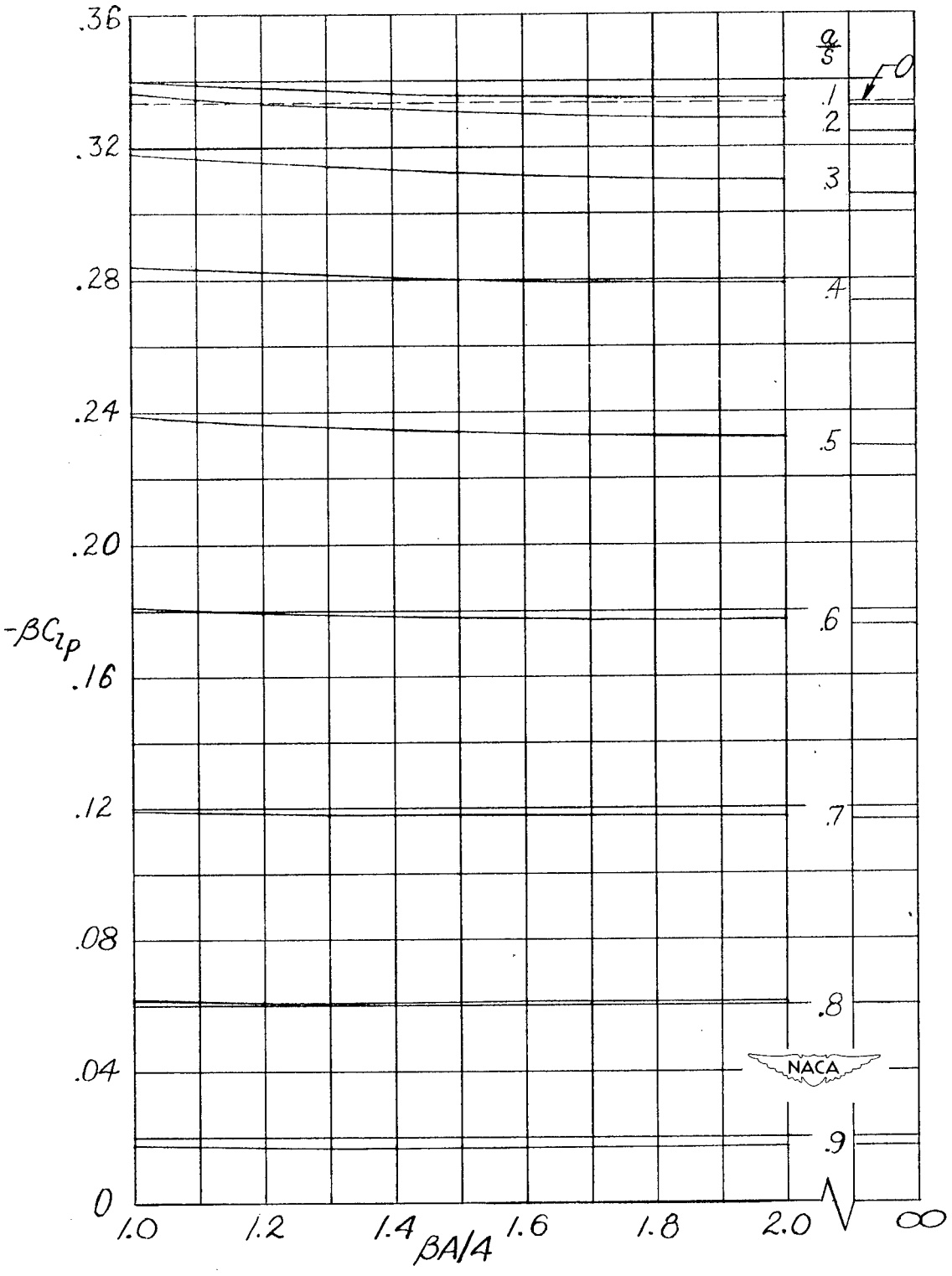

Figure 8.- Damping in roll of triangular wings on cylindrical bodies.

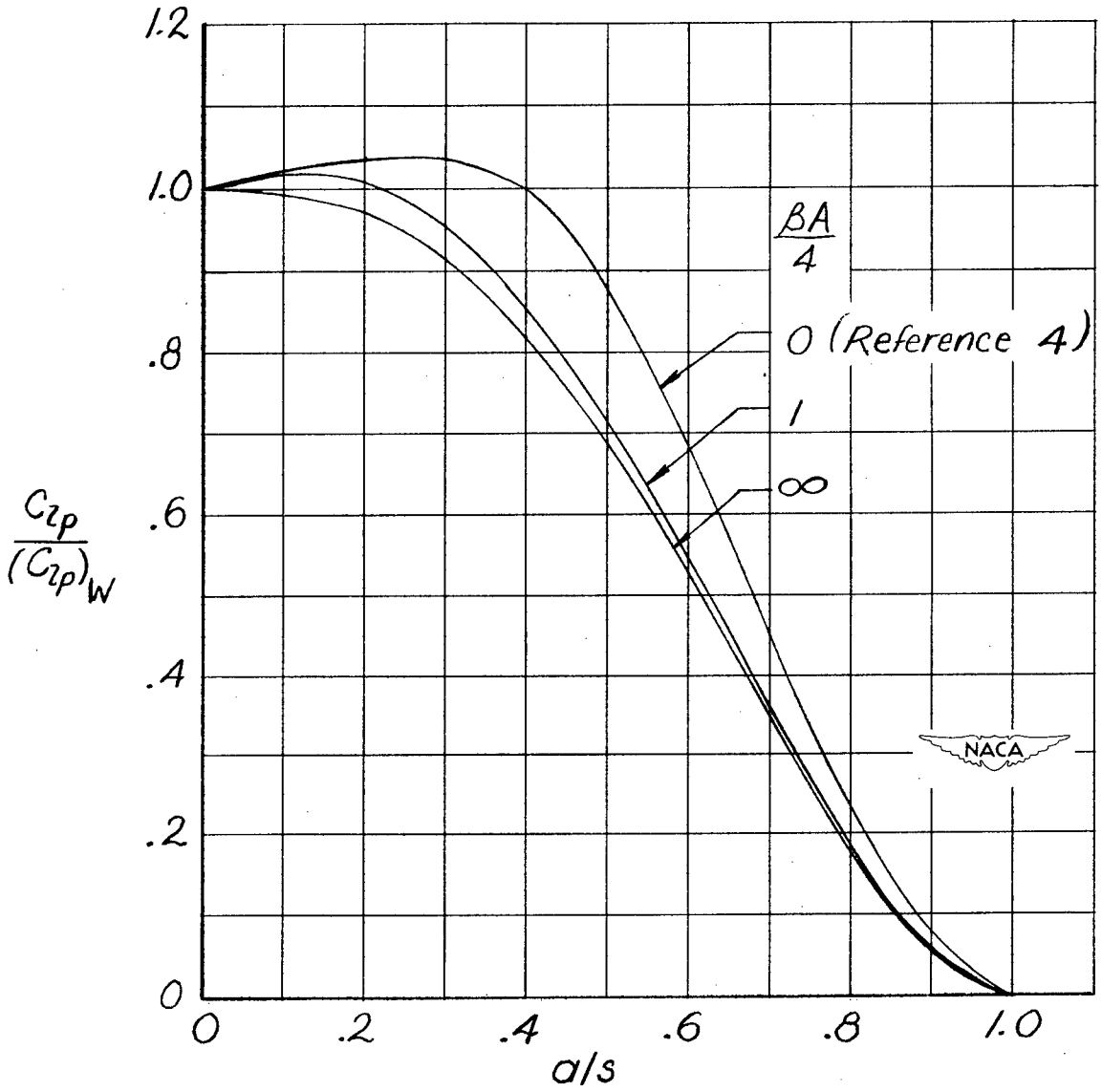

Figure 9.- Relative effect of body for triangular-wing configurations.